Orbital: The Electronic Journal of Chemistry
journal homepage: www.orbital.ufms.br
e-ISSN 1984-6428

| Vol 12 | | No. 3 | | July-September 2020 |

FULL PAPER

Evaluation of Nickel Catalysts Supported in Dry Methane Reform Aiming at Hydrogen Production/Case of Supports: SiO_2, La_2O_3 MCM-41, and Al_2O_3

Paulo Roberto Nagipe da Silva* **and Karine Zanoteli**

Universidade Estadual do Norte Fluminense – UENF, Avenida Alberto Lamego 2000, 28013602 Campos dos Goytacazes – RJ, Brazil.

Article history: Received: 12 May 2020; revised: 10 June 2020; accepted: 17 August 2020. Available online: 28 September 2020. DOI: http://dx.doi.org/10.17807/orbital.v12i3.1495

Abstract:

The importance of biogas was evidenced by the dry reforming reaction using a nickel catalyst supported: Al_2O_3, SiO_2, MCM 41 and La_2O_3. The catalysts were characterized using electron scanning microscopy, Chemisorption, BET, X- Ray analysis. The reaction was conducted in a quartz reactor, atmospheric pressure and at temperatures of 500, 600 and 700 ºC. The catalysts showed different conversions in syngas with the change of temperature, and H_2/CO ratio variable. The nickel catalyst supported on alumina showed the most activity in the three reaction temperatures. The conversion of supported nickel catalysts, in the examined temperatures, decreased in the following order: Ni/Al_2O_3 > Ni/La_2O_3 > $NiSi/O_2$ > Ni/MCM41. The Ni/Al_2O_3 and Ni/MCM-41 catalysts showed H_2/CO greater than one at all temperatures.

Keywords: dry reforming; biogas; nickel catalysts

1. Introduction

The main compounds responsible for the Greenhouse Effect are gases, carbon dioxide, CO_2 and methane, CH_4. Carbon dioxide is emitted mainly by the use of fossil (oil, coal and natural gas) and by various human activities. According to the Intergovernmental Panel on Climate Change, CO_2 is the main "culprit" for global warming, being the gas with the highest emission (approximately 78%) by humans.

Methane gas (CH_4) is produced by the decomposition of organic matter, being abundant in landfills, dumps and hydroelectric reservoirs, and also by livestock (livestock represents 16% of the global emissions of greenhouse gases) and cultivation of rice. In addition, methane is the result of the production and distribution of fossil fuels (gas, oil and coal).

In terms of the degree of dangerousness, it can be seen that methane is more dangerous than CO_2, since it is more efficient in capturing infrared radiation, which causes the Greenhouse effect, than CO_2. The comparative impact of CH_4 on climate change is more than 20 times greater than CO_2, that is, 1 unit of methane is equivalent to 20 units of CO_2.

Sustainable development requires new sources of cheap and renewable energy alternatives for petrochemicals, as well as new approaches to protect the environment, such as the use of greenhouse gas emissions. Biogas is one of the most abundant and versatile sources of energy in the world. It is formed in significant quantities by anaerobic digestion or bacterial fermentation of biomass, or as a result of organic source processing. Biogas is considered a very important source of renewable methane, since it contains (50 - 75%) of it. The second most prevalent component of biogas is carbon dioxide (25 - 50%). Depending on the nature of the primary feed material and its conditions of

*Corresponding author. E-mail: nagipe@uenf.br

sustainable formation it also contains traces of other gases, such as hydrogen sulfide, ammonia, hydrogen, nitrogen, oxygen and water vapor (Table 1) [1-3]. Biogas can be used in several applications. Most of the biogas generated is used to generate heat, mechanical energy and electricity on farms, while the rest is collected in pressurized storage [4, 5].

Table 1. Biogas Composition.

Compound	Formula	%
Methane	CH_4	50-75
Carbon dioxide	CO_2	25-50
Nitrogen	N_2	0-10
Hydrogen	H_2	0-1
Hydrogen sulfide	H_2S	0-3
Oxygen	O_2	0-0

The methane/CO_2 biogas reform may have a potential large-scale application in the production of synthesis gas and hydrogen [6, 7]. Reforming methane with CO_2 can produce synthesis gas with a theoretical H_2/CO ratio of one, which is less than the H_2/CO ratio, obtained by partial oxidation, steam reform, or auto thermal reforming of methane, which generally reach only H_2/CO proportions of 1.7 [8]. A synthesis gas, such as a high CO content, offers the possibility to produce synthesis gas with stoichiometric suitable for certain processes, such as the direct synthesis of aldehydes and alcohols with Oxo synthesis [9, 10] or olefin/gasoline synthesis by Fischer-Tropsch synthesis [11-13].

The catalytic reaction of dry methane reform involves the combination of CH_4 with CO_2, in the presence of a metallic catalyst such as Nickel and temperature (600 - 850 ^oC) to produce synthesis gas (H_2 and CO). This reaction occurs through the stoichiometric balance $CH_4 + CO_2 \rightarrow 2CO + 2H_2$ and has gained increasing interest in promoting the conversion of gases harmful to the environment into fuels and alkane precursors. In addition, it is an important source of hydrogen production.

However, it is known that the greatest limitation for the industrial application of the catalytic dry reform reaction is the deposition of coke, which causes the catalyst to be deactivated and the catalytic reactor to be blocked [14]. Coke formation occurs mainly through the decomposition of CH_4 and the deprotonation of CO. On the other hand, due to the high reaction temperature, the active phase of the catalyst must be dispersed on a support, usually a metal oxide, to provide texture stability and good dispersion of these metals. Therefore, the type of support used is fundamental in the production of a catalytic system with high activity and stability [15, 16].

In this way, the main objective of this work concerns the reform of biogas (CH_4/CO_2) aiming at the production of hydrogen through the use of nickel catalysts supported in several; Al_2O_3, SiO_2, La_2O_3 and MCM-41.

2. Results and Discussion

Table 2 shows the results related to the texture of the catalysts, such as specific surface and pore volume.

Table 2. Results of specific surface and pore volume of the catalysts.

Catalysts	Calcination Temperature (^0C)	Nickel Content Ni%	Specific area (m^2/g)	Pore volume (cm^3/g)
Ni/Si O_2	550	12.9	192	0.52
Ni/MCM-41	500	7.9	205	0.61
Ni/Al_2O_3	500	4.6	123	0.32
Ni/La_2O_3	550	17.5	13.7	0.12

In the X-ray diffractogram of the Ni / Al_2O_3 sample, Figure 1, angles 2θ = 37.10^o were observed; 45.03^o; 59.69^o; these points may be related to the species $NiAl_2O_4$ (nickel aluminate) and the centered face cubic crystalline phase. As previously mentioned, in some catalysts there are interactions between the metal and the support. In the case of nickel catalysts supported on Al_2O_3, NiO, a precursor to the active phase, can react with Al_2O_3, forming nickel aluminate

according to the following reaction:

$NiO + Al_2O_3 \rightarrow NiAl_2O_4 \quad \Delta H = -5,6\ k\ J/mol$

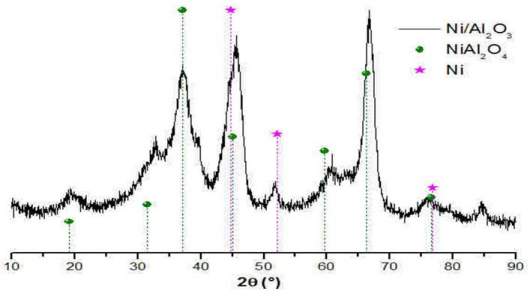

Figure 1. Diffractogram of the Ni/Al_2O_3 catalyst.

The X-ray diffractogram of the MCM-41 catalyst shown in Figure 2 was performed with the material in the form of oxide, after calcination at 700 ^{0}C, for 3 hours. The Ni/MCM-41 analysis is displayed between angles (2θ) from 5 to 90 degrees. For the MCM-41 catalyst, the peaks observed with the presence of the trigonal crystalline phase at 2θ = 37.3^0; 43. 2^0; 6 2. 9^0; 75.4^0; 79.5^0, are related to the species Ni O.

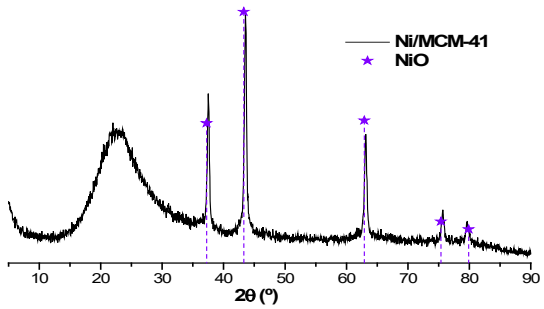

Figure 2. Diffractogram of the Ni / MCM-41 catalyst.

The X - ray diffractogram of the Ni/SiO_2 catalyst in figure 3, was performed with the material in reduced form, after reaction with H_2 at 500 ^{0}C, for 3 hours. The analysis is displayed between angles (2θ) from 5 to 90 degrees.

The diffraction angles: 44.43^o, 51.85^o and 76.23^o in figure 3 indicated the possibility of the cubic phase Ni metallic species, indicated by JCPDS - 010713740.

For this sample, because the non-reduced $NiSiO_2$ material does not exist, and does not have the same support SiO_2 material, it was not possible to perform the XRD analysis of this material.

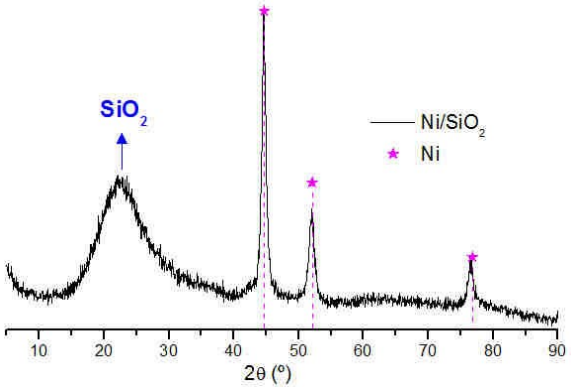

Figure 3. Diffractogram of the Ni/SiO_2 catalyst.

The Ni/La_2O_3 sample was analyzed in the reduced state. The peaks of the X-ray diffractogram, Figure 4, demonstrate the possibility of interaction with the support with the formation of characteristic phases. The phases analyzed in the figure above were related to 2θ = 32.79^0; 47.55^0 and 58.44^0. These angles are characteristic of the NiO phase. The peak referring to the metallic nickel phases could also be observed.

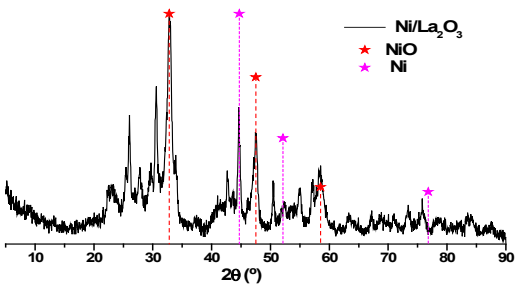

Figure 4. Diffractogram of the Ni/La_2O_3 catalyst.

Through the analysis by scanning electron microscopy - SEM, Figure 5, it can be noticed that the metallic particles are well defined and of heterogeneous size. However, in the case of MCM-41 and SiO_2 samples, a better dispersion of the particles is noticed.

The chemisorption results for the various catalysts are listed in Table 3. In this table, note that the metallic area measurements have a good relationship with the values related to the amount of hydrogen adsorbed. The catalyst that has the smallest measurement of the metallic

area is the Ni/Al_2O_3 catalyst, with 1.7 m^2g^{-1}, the one that adsorbs the least amount of hydrogen 21.4 $\mu molg^{-1}$. On the other hand, the Ni/Al catalyst La_2O_3 has the largest metallic area and the highest amount of adsorbed hydrogen, respectively 3.4 m^2g^{-1} and 43.7 $\mu molg^{-1}$. Regarding dispersion measurements, it is observed that the most loaded nickel catalyst, Ni/La_2O_3, is the one with the lowest dispersion measure, while the least loaded, Ni/Al_2O_3, and has the highest dispersion measure.

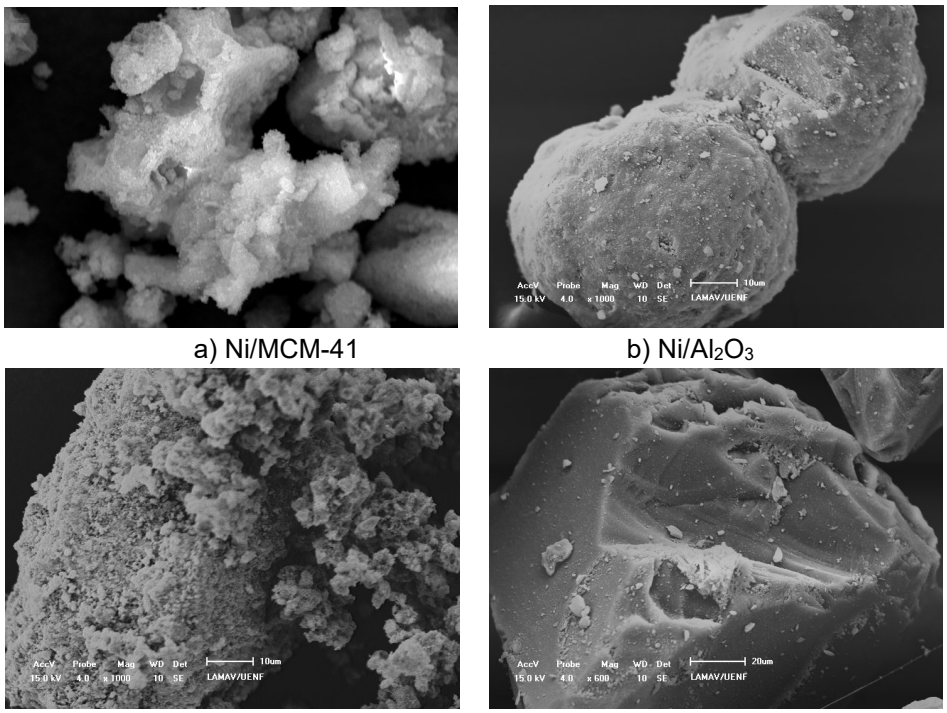

a) Ni/MCM-41 b) Ni/Al_2O_3

c) Ni/La_2O_3 d) Ni/SiO_2

Figure 5. SEM microscopy for nickel catalysts.

Table 3. Results of chemisorption: Nickel content; Metal Dispersion (D); Metallic area and amount of H_2 for Ni catalysts with different supports.

Catalyst	Ni content (%)	Metallic Area (m^2/g)	Dispersion (%)	Amount of H_2 ads. ($\mu mol/g$)
Ni/SiO_2	12.9	3.0	3.0	38.8
Ni/Al_2O_3	4.6	1.7	5.5	21.4
Ni/MCM41	7.9	1.9	3.8	24.8
Ni/La_2O_3	17.3	3.4	2.9	43.7

The results of the biogas reform in the presence of the various catalysts and at temperatures of 500 600 and 700 ^0C are shown in tables 2 - 4. It is observed that all catalysts are active in the Reformation reaction and that the conversion increases with increasing temperature. Figure 6 illustrates the development over time of the conversion of the catalysts. The results of H_2/CO selectivity are also presented; it can be observed that some values less than 1. This fact may be probably due to a possible consumption of H_2 in the process, as a result of the simultaneous occurrence of the reverse reaction of water displacement:

(WGS: $CO_2 + H_2 \rightarrow CO + H_2O$). This is due to the presence of water that is observed at the end of the process.

Values greater than 1 were also observed according to the results in Tables 4-6. In these cases, it can also be observed that the selectivity for CO_2 is greater than for CO. It is possible to admit a large production of hydrogen, observing that in these cases there was a greater formation

of CO_2, and less formation of CO. This occurs in steam reforming of methane. Therefore, water vapor may have formed in the reactor, and it is being consumed in the process, decreasing the amount of CO, by displacing gas water. The selectivity values greater than one occur mainly in the case of the nickel catalyst supported on MCM-41 at all reaction temperatures and then for the nickel catalyst supported on alumina.

Table 4. Results of the biogas reform at 500 ^{0}C.

Catalyst	Ni (%)	C_{CO2}	C_{CH4}	S_{CO}	S_{H2}	H_2/CO
Ni/SiO_2	12.9	42.0	38.0	42.5	33.0	0.77
Ni/Al_2O_3	4.6	76.0	80.0	25.6	28.7	1.12
Ni/MCM-41	7.9	42.0	32.0	13.5	21.7	1.60
Ni/La_2O_3	17.3	70.0	62.0	36.4	32.6	0.89

Table 5. Results of the Biogas Reform at 600 ^{0}C

Catalyst	Ni (%)	C_{CO2} (%)	C_{CH4} (%)	S_{CO} (%)	S_{H2} (%)	H_2/CO
Ni/SiO_2	12.9	60.0	66.0	57.1	56.5	0.99
Ni/Al_2O_3	4.6	82.0	88.0	41.1	65.2	1.60
Ni/MCM-41	7.9	60.0	70.0	46.1	65.2	1.41
Ni/La_2O_3	17.3	66.0	78.0	72.2	66.0	0.91

Table 6. Results of Biogas Reform at 700 ^{o}C.

Catalyst	Ni (%)	C_{CO2} (%)	C_{CH4} (%)	S_{CO} (%)	S_{H2} (%)	H_2/CO
Ni SiO_2	12.9	72.0	88.0	78.8	94.0	1.19
NiAl_2O_3	4.6	86.0	94.0	50.0	89.0	1.78
NiMCM-41	7.9	78.0	92.0	68.2	100	1.47
NiLa_2O_3	17.3	72.0	90.0	76.5	82.8	1.08

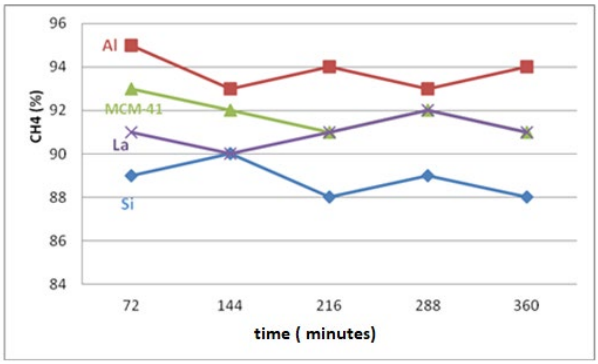

Figure 6. Evolution of catalysts from other nickel-based substrates in the dry reform at 700 ^{0}C in the case of CH_4.

3. Material and Methods

3.1 Preparation of catalysts

The supports used in the development of this work were: SiO_2; Al_2O_3; MCM-41; and La_2O_3. The MCM-41 support was synthesized at the CCT/UENF Catalysis laboratory. While the other supports SiO_2, Al_2O_3 and La_2O_3 are of commercial origin. The supports SiO_2 and Al_2O_3 are from DEGUSSA and lanthanum oxide from VETEC.

The preparation of the catalysts was based on the wet impregnation method (excess solution) for all supports. For this, the nitrate hydrated nickel salt $Ni(NO_3)_2.6H_2O$) was used, where an amount of this salt, relative to obtaining 10% nickel by weight on the catalyst, was placed in solution and put in contact with the support, under constant agitation.

For each impregnation process, the support was stirred with the excess solution of the nickel salt for 12 hours. Then, excess water was removed from the material with heating at 700 ^{o}C, under vacuum, in the rotary evaporator. The sample was kiln - dried for another 12 hours, and then calcined at 500 ^{0}C or 550 ^{0}C for two hours. Some catalysts, such as those for supports SiO_2, La_2O_3 and Al_2O_3, were already pre-prepared for use and, only catalysts were available in reduced form. Therefore, their physical-chemical analyzes were performed with them only in reduced form.

3.2 Characterization of catalysts

The physical-chemical characterization of catalysts is essential, as it makes it possible to explain and predict some of their main properties: activity, selectivity and stability. The physicochemical characterization of catalysts is fundamental, because it makes it possible to explain and predict some of their main properties such as activity, selectivity and stability. Therefore, after the preparation of the catalyst, it becomes necessary to characterize it through the following methods and techniques; chemical analysis, total specific area measurement, X-ray diffraction (XRD), metal area measurement by H_2 chemisorption, X-ray fluorescence (XRF) and scanning electron microscopy (SEM).

The X-ray fluorescence technique was used to determine the chemical composition of the

studied catalysts. In preparing the sample for analysis, a sample powder pellet of about 300 mg was made and analyzed without vacuum. This analysis was performed on the Shimadzu equipment, X-ray Spectrometer EDX-900.

The experiments to evaluate the texture of the catalytic materials were carried out in Quanta chrome Instruments equipment, model Autosorb - 1C. The specific area was determined by the BET method (Brunauet, Emmet and Teller), which involves the analysis of isotherms of physical nitrogen adsorption at various pressures in the temperature of liquid nitrogen.

The X-ray diffractogram of the samples was obtained in a Shimadzu equipment, X-ray Diffractometer XRD - 7000, using radiation, Cu-K α (wavelength = 1.540 Å). The Diffractogram were obtained in the range of 20 to 120º, using a 0.04º step and a counting time of 3 seconds per step. The phases present in the samples were identified with the help of the JCPDS database - Joint Committee on Powder Diffraction Standards. 21 Scanning electron microscopy (SEM) consists of focusing a beam of high energy electrons on the sample in order to obtain an image. The catalysts were analyzed in the SEM equipment of the Shimadzu Model Super Scan SSX-550, with EDS coupled, obtaining secondary electron (SE) images.

The chemical adsorption of H_2 was performed to determine the metallic area of the supported nickel catalysts and nickel dispersion in the prepared catalysts. The sample pre-treatment was carried out in a quartz cell at a temperature of 373 K for two hours to eliminate water. Subsequently, the sample reduction heat treatment was carried out in a hydrogen atmosphere at a temperature of 773 K. After the reduction step, the reactor was isolated, proceeding to lower the temperature to 306 K, the temperature of the chemisorbed hydrogen analysis. The obtained isotherm allows the calculations of the dispersion and metallic area of the supported nickel catalysts.

3.3 Biogas reform

The methane dry reform reaction was carried out in a steel reactor, with a fixed bed, filled with quartz above and below the catalytic bed, formed with 0.100 g of sample. The catalysts were reduced to 500 ^{0}C, under a flow of 30 mLmin^{-1} of H_2 for 1 hour, with a heating speed of 10 ^{o}C min.$^{-1}$. The catalytic tests were conducted in the temperature range of 300 - 1000 ^{0}C, with a gas mixture flow of 60 mL min.$^{-1}$. The simulated biogas used in the process contained the following CH_4 volumetric: CO_2 = 1:1, each with 50% by volume. The reaction took place for six hours and the effluent was analyzed using two different procedures, due to the composition of the effluent gas. A thermal conductivity detector, a component of the chromatographic analysis system for hydrogen detection and analysis, and an infrared detector analysis system for CH_4, CO_2 and CO gases were used. In this case, the gases were collected in special bags and sent to the analysis system by a suction pump coupled to the system.

The chromatographic component temperatures were column 80 ^{0} C, detector temperature: 150 ^{0}C; injector temperature: 120 ^{0}C.

The blueprint of the Reformation reaction scheme is shown in Figure 7.

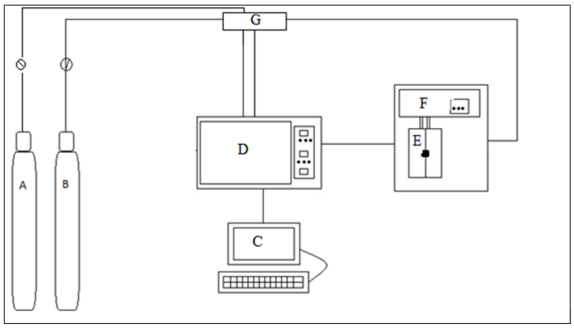

Figure 7. Scheme of the dry methane reform plant. A = biogas cylinder; B = nitrogen gas cylinder; C = computer; D = chromatograph; E = oven; F = temperature regulator and oven heating rate; G = gas valve system.

4. Conclusions

In the preparation of the supported nickel catalysts to be used in the dry methane reforming reaction, the excess impregnation method was used, through the use of a nickel nitrate solution in contact with the support in order to guarantee different levels of metal. Several supports were prepared to highlight the effect of the support on the dry reform reaction. Quantitative RX fluorescence tests indicated

levels consistent with the expected values. This fact indicates that the catalysts were obtained in right preparation conditions.

The different types of supports were found to be in conditions to obtain nickel catalysts with good thermal stability. Thus, the BET method, through physical nitrogen adsorption, guarantees the obtaining of specific varied surfaces and with coherent pore volume distribution.

The distribution of pore sizes for catalysts based on SiO_2, Al_2O_3, MCM-41 and La_2O_3, stands out for a homogeneous behavior for catalysts in the region of 50 - 100 A^0. However, this behavior is altered in the case of the La_2O_3 based catalyst.

The different crystalline phases can be examined through XRD, where we can even identify existing interactions between the metallic phase and the support, as is the case of the nickel alumina interaction, forming the $NiAl_2O_4$ phase. In the case of La_2O_3, the possible interaction with nickel is the NiO phase.

Through electron microscopy analysis it can be seen that as the nickel content increases, an increase in the degree of agglomeration presented by the particles is noticed. On the other hand, it is noted that the particles do not have a homogeneous appearance or well-defined pore size. In the case of MCM-41, Al_2O_3, SiO_2 and La_2O_3 samples, it can be noted that the metallic particles are well defined and of heterogeneous size.

All nickel catalysts showed conversion in the Biogas Reform reaction. Conversions increased with increasing temperature in the 500 - 700 ^{0}C range. On the other hand, the H_2/CO ratio varied for different types of support and with increasing temperature. The catalyst Ni/Al_2O_3 presented itself as the catalyst of greater activity at the temperatures examined sorption, guarantees the obtaining of specific varied surfaces and with coherent pore volume distribution.

The distribution of pore sizes for catalysts based on SiO_2, Al_2O_3, MCM-41 and La_2O_3, stands out for a homogeneous behavior for catalysts in the region of 50 - 100 A^0. However, this behavior is altered in the case of the La_2O_3 based catalyst.

The different crystalline phases can be examined through XRD, where we can even identify existing interactions between the metallic phase and the support, as is the case of the nickel alumina interaction, forming the $NiAl_2O_4$ phase. In the case of La_2O_3, the possible interaction with nickel is the NiO phase.

Through electron microscopy analysis it can be seen that as the nickel content increases, an increase in the degree of agglomeration presented by the particles is noticed. On the other hand, it is noted that the particles do not have a homogeneous appearance or well-defined pore size. In the case of MCM-41, Al_2O_3, SiO_2 and La_2O_3 samples, it can be noted that the metallic particles are well defined and of heterogeneous size.

All nickel catalysts showed conversion in the Biogas Reform reaction. Conversions increased with increasing temperature in the 500 - 700 ^{0}C range. On the other hand, the H_2/CO ratio varied for different types of support and with increasing temperature. The catalyst Ni/Al_2O_3 presented itself as the catalyst of greater activity at the temperatures examined.

References and Notes

[1] Saget, J., “Global CO2 emissions set record in 2010 - IEA” (2011).

[2] Ryckebosch, E.; Drouillon, M. and Vervaeren, H.; *Biomass Bioenergy* **2011**, *35*, 1633. [Crossref]

[3] Qie, S.; Hailong, L.; Jinying, Y.; Longchen, L.; Zhixin Y.; Xinhai Y. *Renewable Sustainable Energy Rev.* **2015**, *51*, 521. [Crossref]

[4] Subramani, V.; Sharma P.; Zhang L.; Liu K.; Song C.; Hydrogen and Syngas Production and Purification Technologies: Hydrocarbon Processing for H_2 Production Eds. K. Liu, C. Song, V. Subramani , Wiley, New-York 2010.

[5] Peng, X. D.; Wang A. W.; Toseland, B. A.; Tijm, P. J. A. *Ind. Eng. Chem. Res.* **1999**, *38*, 4381. [Crossref]

[6] Boll, W.; Supp, E.; Hochgesand, G.; Higman, C.; Kalteie,P. r; Müller, W.D.; Kriebel, M.; Schlichting, H.; and Tanz, Ullmann’s, H.; Encyclopedia of Industrial Chemistry ;Wiley-VCH, Weinheim, 2007, 75.

[7] Wender, I. *Fuel Process. Technol.* **1996**, *48*, 89. [Crossref]

[8] York, A. P. E.; Xiao, T.; Green, M. L. H.; Claridge, J. B. *Catal. Rev.* **2007**, *49*, 511. [Crossref]

[9] Slagtern, A.; Oblbye, U.; Blom, R.; Dahl, I. M.; Fjellvag, H. *Appl. Catal., A* **1996**, *245*, 375. [Crossref]

[10] Valderrama, G.; Goldwasser, M. R.; de Navarro, C. U.; Tatibouet, J. M.; Barraul, J. T.; Batiot Dupeyrat,

C.; Martinez, F. *Catal. Today* **2005**, *107*, 785. [Crossref]

[11] Hu, Y. H.; Ruckenstein, E. *Catal. Lett*. **1996**, *36*, 145. [Crossref]

[12] Tsang, S. C.; Claridge, J. B.; Green, M. L. H. *Catal. Today* **1995**, *23*, 3. [Crossref]

[13] Barroso-Quiroga, M. M.; Castro-Luna, A. E. *Int. J. Hydrogen Energy* **2010**, *35*, 6052. [Crossref]

[14] Pompeo, F.; Nichio, N. N.; Souza, M. M. V. M.; Cesar, D. V.; Ferretti, O. A.; Schmal, M. *Appl. Catal., A* **2007**, *316*, 175. [Crossref]

[15] Gigola, C. E.; Moreno, M. S.; Costilla, I.; Sánchez, M. D. *Appl. Surf. Sci.* **2007**, *254*, 325. [Crossref]

[16] Fakeeha, A. H.; Naeem, M. A.; Khan, W. U.; Al-Fatesh, A. S. *Catalyst Ind. Eng. Chem.* **2014**, *20*, 549. [Crossref]